

## Closed-loop Aspects of Data-Enabled Predictive Control

Dinkla, Rogier; Mulders, Sebastiaan P.; van Wingerden, Jan Willem; Oomen, Tom

**DOI**

[10.1016/j.ifacol.2023.10.1806](https://doi.org/10.1016/j.ifacol.2023.10.1806)

**Publication date**

2023

**Document Version**

Final published version

**Published in**

IFAC-PapersOnLine

**Citation (APA)**

Dinkla, R., Mulders, S. P., van Wingerden, J. W., & Oomen, T. (2023). Closed-loop Aspects of Data-Enabled Predictive Control. *IFAC-PapersOnLine*, 56(2), 1388-1393.  
<https://doi.org/10.1016/j.ifacol.2023.10.1806>

**Important note**

To cite this publication, please use the final published version (if applicable).  
Please check the document version above.

**Copyright**

Other than for strictly personal use, it is not permitted to download, forward or distribute the text or part of it, without the consent of the author(s) and/or copyright holder(s), unless the work is under an open content license such as Creative Commons.

**Takedown policy**

Please contact us and provide details if you believe this document breaches copyrights.  
We will remove access to the work immediately and investigate your claim.

# Closed-loop Aspects of Data-Enabled Predictive Control

Rogier Dinkla\* Sebastiaan P. Mulders\*  
Jan-Willem van Wingerden\* Tom Oomen\*,\*\*

\* *Delft University of Technology, Delft Center for Systems and Control, Mekelweg 2, 2628 CD Delft, The Netherlands (e-mail: r.t.o.dinkla@tudelft.nl).*

\*\* *Eindhoven University of Technology, Control Systems Technology group, De Zaale, 5600 MB Eindhoven, The Netherlands.*

**Abstract:** In recent years, the amount of data available from systems has drastically increased, motivating the use of direct data-driven control techniques that avoid the need of parametric modeling. The aim of this paper is to analyze closed-loop aspects of these approaches in the presence of noise. To analyze this, a unified formulation of several approaches, including Data-enabled Predictive Control (DeePC) and Subspace Predictive Control (SPC) is obtained and the influence of noise on closed-loop predictors is analyzed. The analysis reveals potential closed-loop correlation problems, which are closely related to well-known results in closed-loop system identification, and consequent control issues. A case study reveals the hazards of noise in data-driven control.

Copyright © 2023 The Authors. This is an open access article under the CC BY-NC-ND license (<https://creativecommons.org/licenses/by-nc-nd/4.0/>)

**Keywords:** Data-driven control, subspace predictive control, data-enabled predictive control, closed loop identification, instrumental variables

## 1. INTRODUCTION

The increasing amount of data available from modern systems provides major opportunities for data-driven control. Developments in data-driven models can lead to better performance compared to physical modeling, in particular when these are tuned for control (Markovsky et al., 2022). In the last decades, important aspects regarding the benefits and pitfalls of closed-loop identification have been investigated (Gevers, 2005; Söderstrom and Stoica, 1989; Ljung and McKelvey, 1996; Van den Hof, 1998).

The development of identification for control methods, where the identified model is only used to synthesize a controller, has led to the natural question of whether the identification step can be omitted, leading to a range of direct data-driven control approaches (Markovsky et al., 2022; Hou and Wang, 2013). In Favoreel et al. (1999), Subspace Predictive Control (SPC) is developed, which relies on a linear regression step used in a subspace identification method developed in Van Overschee and De Moor (1994). Further developments include the incorporation of  $H_\infty$  control (Woodley, 2001) and tuning methods to ensure (unconstrained) closed-loop stability (Sedghizadeh and Beheshti, 2018). Recently, in Coulson et al. (2019), the DeePC approach is presented, which relies on Willems' Fundamental Lemma (Willems et al., 2005). DeePC exploits the result that for a linear system, a sufficiently excited past input-output trajectory parameterizes all possible future trajectories (van Waarde et al., 2020). Further developments in the domain of DeePC include closed-loop stability in the presence of measurement noise (Bongard et al., 2022), robust constraint satisfaction (Berberich et al., 2020), extensions to nonlinear systems (Berberich

et al., 2022), and the use of regularization (Coulson et al., 2019) and instrumental variables (van Wingerden et al., 2022) to mitigate the effects of noise.

Although data-driven methods have been well-developed and many successful applications have been reported recently (Markovsky et al., 2022), closed-loop aspects and the implications for control in relation to noise have remained underexposed. However, it seems prudent to consider the effect of closed-loop operation in the presence of noise because the aforementioned data-driven methods inherently operate in closed-loop and often deal with noisy signals. The aim of this paper is to point out potential hazards when applying these direct data-driven control techniques in the presence of noise. In this paper, SPC and DeePC are addressed in a unified fashion, building on the recent results of van Wingerden et al. (2022).

The main contribution of this paper is to provide a closed-loop analysis of a broad class of direct data-driven control algorithms and to point towards potential hazards. A unified framework is established that covers both SPC and DeePC approaches. This paper thereby provides the following contributions:

- (1) A theoretical analysis is performed revealing a closed-loop problem that arises from correlation between inputs and system noise.
- (2) A relevant simulation study clearly illustrates the aforementioned closed-loop problem and shows the resulting impact on performance.
- (3) Suggestions are made to address the closed-loop problem for future work.

## 2. SETUP AND PREREQUISITES

This section introduces the system model, notation, and the assumptions that are used in this paper.

### 2.1 System Model

A discrete-time linear time-invariant (LTI) system description in innovation form is considered, which is also often taken as a basis in subspace identification algorithms (Van Overschee and De Moor, 1996; Knudsen, 2001):

$$x_{k+1} = Ax_k + Bu_k + Ke_k, \quad (1a)$$

$$y_k = Cx_k + Du_k + e_k, \quad (1b)$$

in which  $x_k \in \mathbb{R}^n$ ,  $u_k \in \mathbb{R}^r$ ,  $y_k \in \mathbb{R}^l$ , and  $e_k \in \mathbb{R}^l$  are the respective state, input, output, and (innovation) noise vectors, and  $k \in \mathbb{Z}$  is a discrete-time index. The innovation sequence  $e_k$  is an ergodic zero-mean white noise signal with covariance  $\mathbb{E}[e_k e_j^T] = W\delta_{kj}$ ,  $W > 0$ , and  $\delta_{kj}$  as Kronecker delta function, which is equal to one if  $k = j$  and zero otherwise. The matrices  $A \in \mathbb{R}^{n \times n}$ ,  $B \in \mathbb{R}^{n \times r}$ ,  $C \in \mathbb{R}^{l \times n}$ ,  $D \in \mathbb{R}^{l \times r}$ ,  $K \in \mathbb{R}^{n \times l}$  respectively denote the system, input, Kalman, output and direct feedthrough matrices. By substituting  $e_k$  from (1b) into (1a), the predictor form is obtained

$$x_{k+1} = \tilde{A}x_k + \tilde{B}u_k + Ky_k, \quad (2a)$$

$$y_k = Cx_k + Du_k + e_k, \quad (2b)$$

with  $\tilde{A} = A - KC$ , and  $\tilde{B} = B - KD$ , and where the explicit dependence of the state evolution in (1a) on the noise is replaced by an explicit dependence on the output.

### 2.2 Notation

This section defines the notation that is used throughout this paper. To start,  $I$  and  $0$  are respectively used to indicate an identity matrix and zero matrix of appropriate dimensions.

Block-Hankel matrices are defined as

$$U_{i,s,N} = \begin{bmatrix} u_i & u_{i+1} & \cdots & u_{i+N-1} \\ u_{i+1} & u_{i+2} & \cdots & u_{i+N} \\ \vdots & \vdots & \ddots & \vdots \\ u_{i+s-1} & u_{i+s} & \cdots & u_{i+s+N-2} \end{bmatrix}, \quad (3)$$

with  $i \in \mathbb{Z}$ ,  $\{s, N\} \in \mathbb{Z}^>$ , and  $U_{i,s,N} \in \mathbb{R}^{rs \times N}$ . The block-Hankel matrices  $Y_{i,s,N} \in \mathbb{R}^{ls \times N}$ ,  $E_{i,s,N} \in \mathbb{R}^{ls \times N}$  are defined in a similar manner for the respective outputs and innovations. For the sake of brevity, block-Hankel matrices with only a single block-row omit the second index ( $s = 1$ ), as with states in  $X_{i,N} \in \mathbb{R}^{n \times N}$ .

Block-Toeplitz matrices are defined as

$$\mathcal{T}_s(\mathcal{A}, \mathcal{B}, \mathcal{C}, \mathcal{D}) = \begin{bmatrix} \mathcal{D} & 0 & 0 & \cdots & 0 \\ \mathcal{C}\mathcal{B} & \mathcal{D} & 0 & \cdots & 0 \\ \mathcal{C}\mathcal{A}\mathcal{B} & \mathcal{C}\mathcal{B} & \mathcal{D} & \cdots & 0 \\ \vdots & \vdots & \vdots & \ddots & \vdots \\ \mathcal{C}\mathcal{A}^{s-2}\mathcal{B} & \mathcal{C}\mathcal{A}^{s-3}\mathcal{B} & \cdots & \mathcal{C}\mathcal{B} & \mathcal{D} \end{bmatrix}, \quad (4)$$

with  $\mathcal{A}$ ,  $\mathcal{B}$ ,  $\mathcal{C}$ , and  $\mathcal{D}$  all of compatible dimensions. This definition is used to define  $\mathcal{T}_f^e = \mathcal{T}_f(\mathcal{A}, K, C, I) \in \mathbb{R}^{fl \times fl}$ , and  $\mathcal{T}_f^u = \mathcal{T}_f(\mathcal{A}, B, C, D) \in \mathbb{R}^{fl \times fr}$ , with  $f \in \mathbb{Z}^>$ .

The extended observability matrix of interest is defined by

$$\Gamma_f = [C^T (CA)^T (CA^2)^T \cdots (CA^{f-1})^T]^T \in \mathbb{R}^{fl \times n}. \quad (5)$$

Reversed extended controllability matrices are defined by

$$\mathcal{K}_s(\mathcal{A}, \mathcal{B}) = [\mathcal{A}^{s-1}\mathcal{B} \ \mathcal{A}^{s-2}\mathcal{B} \ \cdots \ \mathcal{A}\mathcal{B} \ \mathcal{B}], \quad (6)$$

with  $\mathcal{A}$  and  $\mathcal{B}$  of appropriate dimensions. This definition is used to define the matrices  $\mathcal{K}_p^u = \mathcal{K}_p(\tilde{A}, \tilde{B}) \in \mathbb{R}^{n \times pr}$  and  $\mathcal{K}_p^y = \mathcal{K}_p(\tilde{A}, K) \in \mathbb{R}^{n \times pl}$ ,  $p \in \mathbb{Z}^>$ .

### 2.3 Assumptions

This paper imposes the below assumptions throughout.

*Assumption 1.* The stationary Kalman gain  $K$  from (1) exists and ensures  $\tilde{A}$  has its eigenvalues strictly inside the unit circle (Anderson and Moore, 1979).

*Assumption 2.* The past window length  $p$  is sufficiently large to ensure that  $\tilde{A}^p \approx 0$ . This is widely used to neglect the effect of an initial state (see also Chiuso (2007)).

*Assumption 3.* The input is assumed to be quasi-stationary to make sure that limits of time averages that use the input sequence exist (Ljung, 1999).

*Assumption 4.* The input is assumed to be sufficiently persistently exciting (Söderstrom and Stoica, 1989).

## 3. UNIFYING SUBSPACE AND DATA-ENABLED PREDICTIVE CONTROL

To provide an analysis that covers a broad class of direct data-driven control algorithms, a unified approach is pursued. To this end, an equivalence between SPC and DeePC in a non-deterministic setting is exposed based on the use of instrumental variables as originally demonstrated in van Wingerden et al. (2022). Both direct data-driven methods are first introduced by explaining several common features.

### 3.1 Commonalities in SPC and DeePC

The setup in Fig. 1 is considered to establish the equivalence. Essentially, SPC and DeePC both solve an optimal control problem in a Model Predictive Control (MPC) framework using an output predictor (Coulson et al., 2019; Favoreel et al., 1999).

To form this output predictor  $\hat{Y}_{i_p, f, 1}$ , from the past data comprising a total length of  $\bar{N}$  data samples, two overlapping sections are used, respectively shown by the green and blue bars. From the green data section, block-Hankel matrices of inputs  $U_{i_p, p, N}$ , and outputs  $Y_{i_p, p, N}$  are constructed with  $p + N - 1 = \bar{N} - f$  samples. Matrices  $U_{i_p, f, N}$  and  $Y_{i_p, f, N}$  are likewise constructed from the blue section, containing  $f + N - 1 = \bar{N} - p$  samples. The sample indices are defined by  $i_p = i + p$ ,  $\hat{i} = i + \bar{N} - p$ , and  $\hat{i}_p = i + \bar{N}$ . Both methods subsequently determine a relationship between data in the green section and data in the blue section. This relationship is then employed to form an output predictor  $\hat{Y}_{i_p, f, 1}$  that is dependent on some past input-output data  $U_{i_p, 1}^y$  and  $Y_{i_p, 1}^y$  as well as future inputs  $U_{i_p, f, 1}^u$ . These future inputs are optimized given the cost function, a reference trajectory  $r_f$ , and the output predictor.

### 3.2 The data equation

To establish an equivalence note that the different methods use past data trajectories for controller synthesis. The aim

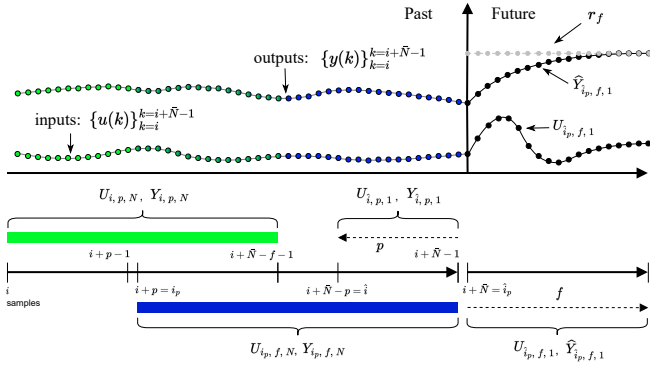


Fig. 1. SPC and DeePC controller synthesis principles: two (overlapping, in green and blue) past input-output trajectories are used to form an output predictor  $\widehat{Y}_{i_p, f, 1}$  with which to optimize future inputs  $U_{i_p, f, 1}$  in a receding horizon setting given reference  $r_f$ .

of this section is to provide the data equations that capture the system behaviour in terms of these past input-output trajectories.

The first step involves the dependence of the block-Hankel matrix of past outputs  $Y_{i_p, f, N}$  from Fig. 1 in terms of past inputs  $U_{i_p, f, N}$  and  $U_{i_p, N}$ , and past outputs  $Y_{i_p, N}$ . By propagating the innovation model (1)  $f-1$  steps forwards in time from initial state  $x_{i_p}$ , the leftmost column of

$$Y_{i_p, f, N} = \Gamma_f X_{i_p, N} + \mathcal{T}_f^u U_{i_p, f, N} + \mathcal{T}_f^e E_{i_p, f, N} \quad (7)$$

is obtained. The complete equation is constructed by horizontal concatenation of the column vectors that result from each of the  $N$  consecutive initial states in  $X_{i_p, N}$ .

Equation (7) does not yet indicate the dependence of  $Y_{i_p, f, N}$  on  $Y_{i_p, N}$  and  $U_{i_p, N}$ . Considering the predictor form (2) it is clear that the states  $X_{i_p, N}$  can however be rewritten in terms of the past inputs  $U_{i_p, N}$  and outputs  $Y_{i_p, N}$  as well as a new set of initial states  $X_{i, N}$ . As such, considering that  $i_p = i+p$ , propagate (2a)  $p$  steps forwards in time from the initial states in  $X_{i, N}$  to find

$$X_{i_p, N} = \tilde{A}^p X_{i, N} + \mathcal{K}_p^u U_{i_p, N} + \mathcal{K}_p^y Y_{i_p, N}. \quad (8)$$

By substituting (8) in (7) it is then found that

$$Y_{i_p, f, N} = \begin{bmatrix} \Gamma_f \mathcal{K}_p & \mathcal{T}_f^u \\ U_{i_p, f, N} \end{bmatrix} \begin{bmatrix} Z_N \\ U_{i_p, f, N} \end{bmatrix} + \mathcal{T}_f^e E_{i_p, f, N} + \Gamma_f \tilde{A}^p X_{i, N}, \quad (9)$$

where in the interest of brevity we define  $\mathcal{K}_p = \begin{bmatrix} \mathcal{K}_p^y & \mathcal{K}_p^u \end{bmatrix}$  and  $Z_N^T = [Y_{i_p, N}^T \ U_{i_p, N}^T]$ . Equation (9) is commonly referred to as the *data equation*, and it is fundamental to the use of DeePC and SPC. The way in which the output predictor is formed is explained next.

### 3.3 Obtaining the output predictor

The distinguishing feature between SPC and DeePC is how a relationship is inferred from the past data to arrive at an output predictor. This section first illustrates this process for SPC and then for DeePC.

**Subspace Predictive Control (SPC):** Given the stochastic nature of the innovation sequence, note that the structure

of the data-equation (9) lends itself well to a linear least-squares estimation problem of  $[\Gamma_f \mathcal{K}_p \ \mathcal{T}_f^u]$ , which will be referred to as the dynamic matrix. In fact, the output predictor that SPC uses is of the form

$$\widehat{Y}_{i_p, f, 1} = \widehat{[\Gamma_f \mathcal{K}_p \ \mathcal{T}_f^u]} \begin{bmatrix} z_p \\ U_{i_p, f, 1} \end{bmatrix}, \quad (10)$$

in which the circumflex notation  $\widehat{(\cdot)}$  is used to indicate an estimate and a past data vector is defined as  $z_p^T = [Y_{i_p, N}^T \ U_{i_p, N}^T]$  for brevity. The contribution of the initial states is neglected by means of Assumption 2.

The dynamic matrix estimate in (10) is obtained by solving

$$\widehat{[\Gamma_f \mathcal{K}_p \ \mathcal{T}_f^u]} = \arg \min_L \|Y_{i_p, f, N} - L \bar{Z}_N\|_F^2, \quad (11)$$

with  $L \in \mathbb{R}^{f \times p(r+l)+fr}$  to be optimized,  $\|\cdot\|_F$  indicating a Frobenius norm, and  $\bar{Z}_N^T = [Z_N^T \ U_{i_p, f, N}^T]$ . The analytical solution to the above estimation problem is

$$\widehat{[\Gamma_f \mathcal{K}_p \ \mathcal{T}_f^u]} = \frac{1}{N} Y_{i_p, f, N} \bar{Z}_N^T \left( \frac{1}{N} \bar{Z}_N \bar{Z}_N^T \right)^{-1}, \quad (12)$$

in which Assumption 4 ensures that the inverse exists. The fractions preceding matrix products above are superfluous since they cancel, but serve as a reminder that in a non-deterministic setting the estimate is based on empirical correlation matrices (Van Overschee and De Moor, 1996). Assumption 3 ensures that the empirical correlation matrices above approach a well-defined actual correlation matrix as  $N \rightarrow \infty$ .

Combining (10) with (12) the output predictor becomes

$$\widehat{Y}_{i_p, f, 1} = Y_{i_p, f, N} \bar{Z}_N^T \left( \bar{Z}_N \bar{Z}_N^T \right)^{-1} \begin{bmatrix} z_p \\ U_{i_p, f, 1} \end{bmatrix}. \quad (13)$$

**Data-enabled Predictive Control (DeePC):** The output predictor is determined in a different way in DeePC, as the algorithm makes use of Willems' Fundamental Lemma. Providing Assumption 4 is satisfied, in a noise-free setting, linear combinations of past input-output trajectories characterize all feasible future input-output trajectories. However, in the non-deterministic case, the above characterization is imperfect because the trajectories are corrupted by noise. In van Wingerden et al. (2022) instrumental variables are employed to mitigate the effects of this noise, which is the approach also followed here.

To this end, the linear combination of past input-output trajectories is restricted to lie in the row-space of  $\bar{Z}_N$ , which functions as an *instrumental variable* because it is assumed to be uncorrelated with the noise and is highly correlated with the data matrix  $\bar{Z}_N$  – which in this case is itself. This results in an output predictor described by

$$\begin{bmatrix} z_p \\ U_{i_p, f, 1} \end{bmatrix} = \bar{Z}_N \bar{Z}_N^T g, \quad (14a)$$

$$\widehat{Y}_{i_p, f, 1} = Y_{i_p, f, N} \bar{Z}_N^T g, \quad (14b)$$

in which  $g \in \mathbb{R}^{p(l+r)+fr}$  is a vector. Assumption 4 ensures that (14a) permits a unique solution for  $g$ , which when substituted in (14b) obtains (13) as output predictor.

Since DeePC and SPC share the same output predictor in a non-deterministic setting using instrumental variables, given the same noise realizations, cost function, and constraints, the analytical solutions are equivalent. Hence,

whilst the closed-loop identification problem is derived next in the context of SPC, it also applies to DeePC.

#### 4. CLOSED-LOOP IDENTIFICATION PROBLEM

In this section, the unified setup of Section 3 is employed to investigate closed-loop aspects in direct data-driven control. To compute the output predictor, both SPC and DeePC implicitly assume that the instrumental variable  $\bar{Z}_N = [Y_{i,p,N}^T \ U_{i,p,N}^T \ U_{i,p,f,N}^T]^T$  is uncorrelated with the noise. This assumption is clearly violated when the input-output data has been acquired from closed-loop operation, as is inherently the case with SPC and DeePC; the controller determines inputs in part from measured outputs, which in turn are affected by noise as shown by (2b).

##### 4.1 Operational modes

The nature of the correlation between inputs and noise depends on how frequently the controller is updated since different controllers logically induce different correlations. Hence, three different operational modes are discerned below given an initial sufficiently exciting past input-output trajectory obtained from open-loop operation.

- (1) *Non-adaptive operation:* The initial open-loop data is used to form an output predictor and thereby synthesize a controller. Thereafter, the output predictor, and thus the controller, remains the same.
- (2) *Adaptive operation:* Under adaptive operation, correlation between inputs and system noise under feedback are a result of multiple different controllers.
- (3) *Batch-wise operation:* The controller is updated (at most) once every  $\bar{N}$  samples. Hence, a new controller works with input-output trajectories that have been affected only by the directly preceding controller.

With adaptive operation a mechanism that affects correlation between inputs and noise under feedback is the stochastic variability of the different controllers. In batch-wise operation the closed-loop correlation between inputs and noise experienced during controller synthesis comes only from the preceding controller, which simplifies the analysis. Hence, the analysis presented in the remainder of this paper employs batch-wise operation.

##### 4.2 The closed-loop identification problem

In this section the bias that is introduced due to correlation between inputs and noise is derived along the lines of the consistency analysis in Knudsen (2001) using the data equation (9) and the SPC framework.

The actually obtained future outputs that are estimated by the output predictor are given akin to (9) as

$$Y_{i,p,f,1} = [\Gamma_f \mathcal{K}_p \ \mathcal{T}_f^u] \begin{bmatrix} z_p \\ U_{i,p,f,1} \end{bmatrix} + \mathcal{T}_f^e E_{i,p,f,1} + \Gamma_f \tilde{A}^p X_{i,1}. \quad (15)$$

The resulting error of the output predictor is found by subtracting (15) from (10) to find that

$$\begin{aligned} \hat{Y}_{i,p,f,1} - Y_{i,p,f,1} = & \\ & \left[ \widehat{[\Gamma_f \mathcal{K}_p \ \mathcal{T}_f^u]} - [\Gamma_f \mathcal{K}_p \ \mathcal{T}_f^u] \right] \begin{bmatrix} z_p \\ U_{i,p,f,1} \end{bmatrix} \\ & - \mathcal{T}_f^e E_{i,p,f,1} - \Gamma_f \tilde{A}^p X_{i,1}. \end{aligned} \quad (16)$$

The bias of the output predictor is given by the expected value of this error, which using Assumption 2 reduces to the expected value of the middle row. Clearly, the bias of the estimated dynamic matrix plays a significant role in the bias of the output predictor. To find the error of the estimated dynamic matrix substitute (9) in (12) and subtract the actual dynamic matrix to find

$$\begin{aligned} \left[ \widehat{[\Gamma_f \mathcal{K}_p \ \mathcal{T}_f^u]} - [\Gamma_f \mathcal{K}_p \ \mathcal{T}_f^u] \right] = & \\ & \mathcal{T}_f^e \left( \frac{1}{N} E_{i,p,f,N} \bar{Z}_N^T \right) \left( \frac{1}{N} \bar{Z}_N \bar{Z}_N^T \right)^{-1} \\ & + \Gamma_f \tilde{A}^p \left( \frac{1}{N} X_{i,N} \bar{Z}_N^T \right) \left( \frac{1}{N} \bar{Z}_N \bar{Z}_N^T \right)^{-1}. \end{aligned} \quad (17)$$

Whilst, as before, the bottom row will vanish under Assumption 2, the middle row requires the empirical correlation matrix  $E_{i,p,f,N} \bar{Z}_N^T / N$  to vanish<sup>1</sup>. The instrumental variable  $\bar{Z}_N$  contains inputs  $U_{i,p,f,N}$ , which in closed-loop will be determined in part by outputs and hence noise  $E_{i,p,f,N}$ . This in turn means that the input and noise sequences are correlated, which as (17) demonstrates prevents unbiased estimation of the dynamic matrix  $[\Gamma_f \mathcal{K}_p \ \mathcal{T}_f^u]$  even as both  $p, N \rightarrow \infty$ .

The bias that is encountered is problematic because it degrades the accuracy of the output predictor as demonstrated by (16), thereby potentially reducing the performance of adaptive or batch-wise SPC and DeePC implementations in the presence of noise.

## 5. SIMULATION RESULTS

This section presents several batch-wise, unconstrained SPC simulation results that demonstrate the existence of correlation between inputs and noise when using data obtained in closed-loop, resulting in a bias of the estimated dynamic matrix and thus performance degradation of the considered data-driven control methods.

To illustrate these effects the 5<sup>th</sup> order, marginally stable system from Favoreel et al. (1999) (representing a motor that drives two plates and flexible shafts) is simulated. Batch-wise SPC operation is simulated using equal past and future window lengths  $p = f = 50$ , which is common in subspace methods (van der Veen et al., 2013), for 24 different numbers of columns  $N$  ranging from 180 to 8459. For each  $N$ , 120 different noise realizations are taken to obtain averaged quantities of interest.

### 5.1 Batch-wise simulation

The batch-wise simulation procedure is illustrated by Fig. 2. For each noise realization, the simulation is performed for three consecutive sections of equal length ( $\bar{N} = p + f + N - 1$ ). The zero-mean white noise innovation sequence of the system as given by (1) has  $\text{var}(e_k) = 0.01$  for all three of the sections. In the first section, the input is a zero-mean white noise signal with  $\text{var}(u_k) = 1$  to provide a persistently exciting input with which to initialize a controller that is based on open-loop data. From this point onwards, the input is determined by the controller and a zero mean white-noise input disturbance  $d_k$  with  $\text{var}(d_k) = 0.05$ . This considerably smaller

<sup>1</sup> In Peternell et al. (1996) it is additionally shown that consistent estimation of the estimated matrix requires that  $N$  must go to infinity at an adequately larger rate than  $p$  goes to infinity.

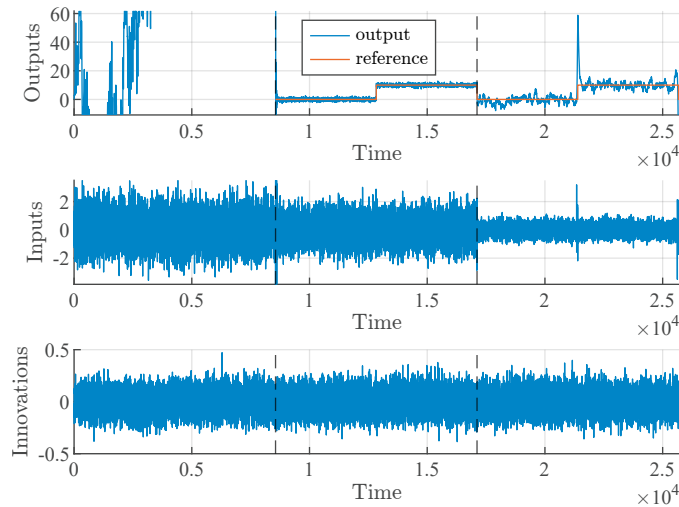


Fig. 2. Illustration of a data-driven control pitfall in closed-loop using  $N = 8459$ . The reference-tracking performance of the updated controller is considerably reduced due to identification bias arising from correlation between inputs and noise in closed-loop.

variance of the stochastic input component is chosen to guarantee satisfaction of Assumption 4 whilst maintaining a similar input variance as in the first section. Henceforth, the controller tracks a reference with a step magnitude of 10. Based on the resulting closed-loop input-output data from the second section the controller is subsequently updated again. The last section serves to illustrate the performance of batch-wise operation using closed-loop data, but its data is not processed further in this paper. That is, except for Fig. 2, the results shown here only consider the closed-loop data from the second section.

Moreover, since closed-loop stability is not ensured, only noise realizations that lead to a closed-loop stable system are used. This is necessary to satisfy Assumption 3 and hence demonstrate meaningful correlations between inputs and noise. Similarly, to satisfy Assumption 4, only noise realizations that lead to a full row rank  $\bar{Z}_N$  are used.

### 5.2 Correlation between inputs and noise

Fig. 3 illustrates the correlation that arises between inputs and noise in closed-loop, and shows the correlation matrix  $E_{i_p,f,N} \bar{Z}_N^T / N$  from (17) for  $N = 8459$  as averaged over the 120 noise realizations. The data that was obtained in open-loop indicates no significant correlation. However, the data that was obtained in closed-loop in the subsequent section of the simulations clearly shows a causal correlation that arises between the relevant input and innovation signals. The correlation is illustrated for the maximum number of columns that was investigated ( $N = 8459$ ) because under such conditions experimental correlation matrices best reflect the actual correlation.

To quantify the correlation between the inputs and the noise  $E_{i_p,f,N} U_{i_p,f,N}^T / N$  a squared Frobenius norm is used. The resulting plot is shown by Fig. 4. This figure clearly shows that in open-loop, the experimental correlation decreases with  $N$ . This is to be expected since in open-loop these inputs are uncorrelated with the innovation

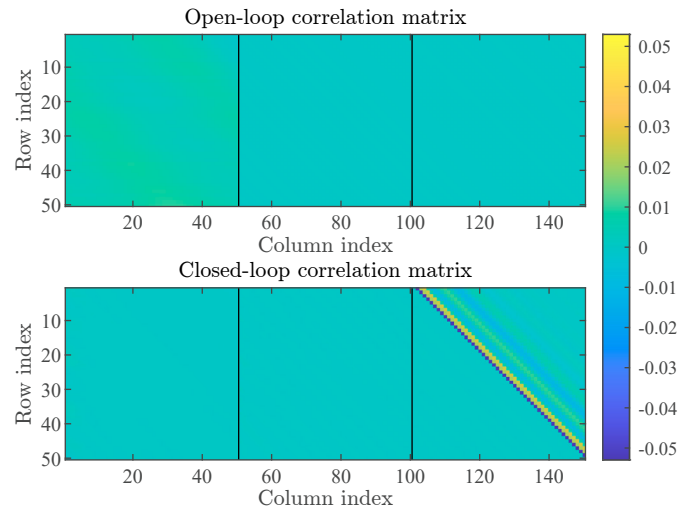


Fig. 3. Visualization of the average open and closed-loop correlation matrices  $E_{i_p,f,N} \bar{Z}_N^T / N$  for  $N = 8459$ . Note the non-zero, causal closed-loop correlation between future inputs and noise.

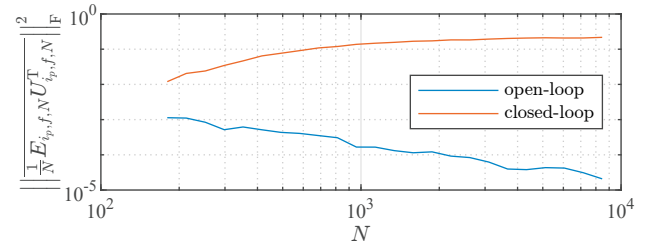


Fig. 4. Squared Frobenius norm of the average open and closed-loop matrices  $E_{i_p,f,N} U_{i_p,f,N}^T / N$  for varying  $N$ . Uncorrelated signals should display a correlation that decreases with  $N$ , which is not visible for the closed-loop correlation between inputs and noise shown here.

sequence. In closed-loop however, existing correlation between inputs and noise becomes evident as the number of columns  $N$  increases. As described this is due to the fact that in closed-loop, inputs from the controller are based on past outputs, which in turn are affected by noise.

### 5.3 Bias of the dynamic matrix estimate

Equation (17) indicates that in closed-loop a bias is introduced in the estimation of the dynamic matrix as a result of the correlation between inputs and noise. This holds true even if  $p$  is sufficiently large. Fig. 5 illustrates the open-loop and closed-loop bias for different values of  $N$  and the different components of the estimate of the dynamic matrix  $[\Gamma_f \mathcal{K}_p \mathcal{T}_f^u] = [\Gamma_f \mathcal{K}_p^y \Gamma_f \mathcal{K}_p^u \mathcal{T}_f^u]$ .

For data obtained in open-loop, the results in Fig. 5 are illustrative of consistent estimation, meaning that the bias decreases asymptotically with increasing  $N$  (Söderstrom and Stoica, 1989). In this case it is expected that the bias would eventually approach a limit that is determined by the contribution of a finite  $p$  apparent from (17). Moreover, Fig. 5 demonstrates that the bias of the different estimated matrix components deriving from closed-loop operation actually increase with  $N$  (at least after some initial value in the case of the two leftmost plots).

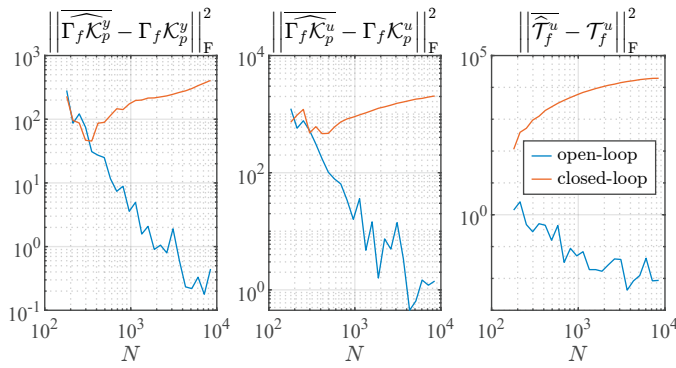


Fig. 5. Squared Frobenius norm of the error of different average open and closed-loop matrix estimates (used to quantify estimation bias) for varying  $N$ . Since the bias of the closed-loop estimates does not decrease asymptotically these estimates are not consistent.

#### 5.4 Impact on controller performance

The biased estimate of the dynamic matrix  $[\Gamma_f \mathcal{K}_p \mathcal{T}_f^u]$  deriving from closed-loop operation clearly introduces a bias in the output predictor according to (16). The biased predictor in turn has an impact on the performance of the controller as it is used in an MPC setting. Fig. 2 serves as an example of how closed-loop system identification in a direct data-driven control framework can degrade the performance of a reference-tracking controller.

## 6. CONCLUSION

The theoretical and simulation results of this paper reveal that direct data-driven control may suffer from identification bias arising from closed-loop correlation between inputs and noise. This bias can impact the performance, potentially even leading to closed-loop instability. Whilst results here are presented using SPC, based on the derived unified framework, it is clear that the closed-loop problem is also to be expected with other direct data-driven methods like DeePC. In the future we intend to investigate two promising solution methods in the contexts of SPC and DeePC. These methods respectively avoid close-loop correlation by means of a past window length  $f = 1$  (Ljung and McKelvey, 1996) or the use of instrumental variables (Söderstrom and Stoica, 1989).

## REFERENCES

Anderson, B.D. and Moore, J.B. (1979). *Optimal Filtering*. Prentice Hall, Englewood Cliffs, New Jersey.

Berberich, J., Köhler, J., Müller, M.A., and Allgöwer, F. (2020). Robust Constraint Satisfaction in Data-Driven MPC. In *2020 59th IEEE Conference on Decision and Control (CDC)*, 1260–1267.

Berberich, J., Köhler, J., Müller, M.A., and Allgöwer, F. (2022). Linear Tracking MPC for Nonlinear Systems—Part II: The Data-Driven Case. *IEEE Transactions on Automatic Control*, 67(9), 4406–4421.

Bongard, J., Berberich, J., Koehler, J., and Allgöwer, F. (2022). Robust stability analysis of a simple data-driven model predictive control approach. *IEEE Transactions on Automatic Control*.

Chiuso, A. (2007). The role of vector autoregressive modeling in predictor-based subspace identification. *Automatica*, 43(6), 1034–1048.

Coulson, J., Lygeros, J., and Dörfler, F. (2019). Data-Enabled Predictive Control: In the Shallows of the DeePC. In *2019 18th European Control Conference (ECC)*, 307–312. IEEE, Naples, Italy.

Favoreel, W., De Moor, B., and Gevers, M. (1999). SPC: Subspace Predictive Control. *IFAC Proceedings Volumes*, 32(2), 4004–4009.

Gevers, M. (2005). Identification for Control: From the Early Achievements to the Revival of Experiment Design. *European Journal of Control*, 11(4), 335–352.

Hou, Z.S. and Wang, Z. (2013). From model-based control to data-driven control: Survey, classification and perspective. *Information Sciences*, 235, 3–35.

Knudsen, T. (2001). Consistency analysis of subspace identification methods based on a linear regression approach. *Automatica*, 37(1), 81–89.

Ljung, L. (1999). *System Identification: Theory for the User*. Prentice Hall, second edition.

Ljung, L. and McKelvey, T. (1996). Subspace identification from closed loop data. *Signal Processing*, 52(2), 209–215.

Markovskiy, I., Huang, L., and Dörfler, F. (2022). Data-driven control based on behavioral approach: From theory to applications in power systems. *IEEE Control Systems*.

Peternell, K., Scherrer, W., and Deistler, M. (1996). Statistical analysis of novel subspace identification methods. *Signal Processing*, 52(2), 161–177.

Sedghizadeh, S. and Beheshti, S. (2018). Data-driven subspace predictive control: Stability and horizon tuning. *Journal of the Franklin Institute*, 355(15), 7509–7547.

Söderstrom, T. and Stoica, P. (1989). *System Identification*. Prentice Hall.

Van den Hof, P. (1998). Closed-loop issues in system identification. *Annual Reviews in Control*, 22, 173–186.

van der Veen, G., van Wingerden, J.W., Bergamasco, M., Lovera, M., and Verhaegen, M. (2013). Closed-loop subspace identification methods: An overview. *IET Control Theory & Applications*, 7(10), 1339–1358.

Van Overschee, P. and De Moor, B. (1994). N4SID: Subspace Algorithms for the Identification of Combined Deterministic-Stochastic Systems. *Automatica*, 30(1), 75–93.

Van Overschee, P. and De Moor, B. (1996). *Subspace Identification for Linear Systems*. Springer US, Boston.

van Waarde, H.J., De Persis, C., Camlibel, M.K., and Tesi, P. (2020). Willems’ Fundamental Lemma for State-Space Systems and Its Extension to Multiple Datasets. *IEEE Control Systems Letters*, 4(3), 602–607.

van Wingerden, J.W., Mulders, S.P., Dinkla, R., Oomen, T., and Verhaegen, M. (2022). Data-enabled predictive control with instrumental variables: The direct equivalence with subspace predictive control. In *2022 IEEE 61st Conference on Decision and Control (CDC)*, 2111–2116. Cancun, Mexico.

Willems, J.C., Rapisarda, P., Markovskiy, I., and De Moor, B.L. (2005). A note on persistency of excitation. *Systems & Control Letters*, 54(4), 325–329.

Woodley, B.R. (2001). *Model Free Subspace Based  $H_\infty$  Control*. Ph.D. thesis, Stanford University.